Engineering Applications of Artificial Intelligence 127 (2024) 107264

Contents lists available at ScienceDirect

Engineering Applications of Artificial Intelligence

journal homepage: www.elsevier.com/locate/engappai

A lane-changing trajectory re-planning method considering conflicting traffic scenarios

Haifeng Du [a], Yu Sun [a], Yongjun Pan [a,*], Zhixiong Li [b], Patrick Siarry [c]

[a] State Key Laboratory of Mechanical Transmission, College of Mechanical and Vehicle Engineering, Chongqing University, Chongqing, China
[b] Faculty of Mechanical Engineering, Opole University of Technology, Opole, 45758, Poland
[c] University Paris-Est Créteil Val de Marne, 61 Av. du General de Gaulle, 94010, Creteil, France

ARTICLE INFO

Keywords:
Lane change
Collision avoidance
Trajectory re-planning
Neural network

ABSTRACT

An essential aspect of intelligent driving systems is the automatic lane-changing function. However, in real-world traffic situations, the initially planned lane-changing trajectory can become hazardous due to the intricate and unpredictable nature of human driving behavior. Based on the assumption that vehicles have risks during lane-changing, an integrated methodology is proposed to assess the hazards associated with road conditions in real-time and to quickly adjust the predetermined vehicle trajectory, if deemed necessary, to mitigate the risks of conflicting lane changes. Vehicles are encouraged to adhere to lane changing behavior by adjusting their trajectory, aiming to enhance traffic efficiency. Instead of immediately abandoning lane changing, vehicles should strategically assess the situation before making decisions. Initially, an analysis of variables influencing re-planning is conducted, determining the circumstances conducive to maintaining lane-changing behavior. Subsequently, a trajectory re-planning module is introduced, facilitated by two neural network data-fitting models, allowing real-time performance. Finally, a series of numerical experiments confirm that the devised method effectively guides autonomous driving through quick and secure lane change re-planning in high-risk traffic environments. The proposed novel approach extends the capacity to target traffic flow gaps and dynamically re-plan lane switching motivations, ensuring the vehicle can persist in lane-changing rather than reverting to the original lane.

1. Introduction

Recently, with the rise of artificial intelligence, intelligent vehicles have also achieved rapid development with equipped technologies for automation and wireless connectivity. Among the various functions of the intelligent driving system, the automatic lane-changing (LC) sub-system that takes charge of the safe and effective LC receives a great deal of interest and extensive research in the domestic and overseas (Rahman et al., 2013). Most researchers currently believe that the LC automatic system consists of four main characters: awareness of the environment, decision-making, trajectory planning and motion control (Guanetti et al., 2018; Schwarting et al., 2018). Serving as a fundamental and universal component of the autonomic driving system, the environment awareness module leverages insightful information from onboard sensors, wayside detection devices and vehicle communication to describe the driving environment. The description is required to be completed in a timely and effective manner and conveyed to all intelligent submodules. In terms of LC decision making, it refers to the use of rule judgment, big data fitting, and other methods to determine if a vehicle is suitable for implementing LC behavior given a specific traffic scenario and driving goal. Then under the premise that the decision-making module issues the LC instruction with target lanes, an optimal trajectory would be generated by the trajectory planning algorithm given the performance goals of safety, comfort, fuel economy, and driving stability, *etc.* Ultimately, the trajectory is input as a reference line to the vehicle's dynamics module for the path-tracking control containing information about the vehicle's position, velocity, and yaw states. The four modules are highly correlated with each other, and a full automatic LC operation requires performing them all correctly.

To date, many researchers have presented their conceptions of trajectory planning for the smart LC system. There are several curve designs in the process of trajectory planning, falling mainly into three broad categories: spiral curves (Bae et al., 2022), Bezier curves (Yang et al., 2022b), and polynomial curves (Ding et al., 2021). Among the path curves, the quintic polynomial is the simplest and most widely

* Corresponding author.
E-mail address: yongjun.pan@cqu.edu.cn (Y. Pan).

https://doi.org/10.1016/j.engappai.2023.107264
Received 20 April 2023; Received in revised form 28 September 2023; Accepted 3 October 2023
Available online 14 October 2023

used polynomial that enjoys the benefits of curvature continuity, a simple implementation, and fast computation. The curve can be simplified to discrete points and coupled to Model Predictive Controller (MPC) to achieve LC operations (Kim et al., 2023). Then, the trajectory is required to be optimized for practical applicability in accordance with the performance indicators of safety, comfort, fuel economy, and driving stability. The optimization function is commonly and correspondingly constructed related to the vehicle parameters of velocity, acceleration, jerk, and vibration (Chen et al., 2022; Ding et al., 2021; Li et al., 2022a). Significantly, the safety assurance during LC must be carefully considered and is typically manifested by the constraints of safety distance (Maleki et al., 2022), artificial potential field (Yan et al., 2022), aggressiveness index (Hu et al., 2022), and so on. Multiple optimization methods have been proposed and applied to the improvement of LC process. Zhang et al. employed the Technique for Order Preference by Similarity to Ideal Solution (TOPSIS) for trajectory optimization (Zhang et al., 2022b). Wang et al. further combined the TOPSIS with the Non-Dominated Sorting Genetic Algorithm II (NSGA-II) and achieved great results (Wang et al., 2023). In Yang et al. (2022a) and Typaldos et al. (2022), the trajectory determination problem was characterized and treated in the form of a non-convex quadratic-constrained quadratic programming (QP) problem. Ajanović et al. integrated search-based task and motion planning for hybrid systems (Ajanović et al., 2023).

However, in the real context of mixed-autonomy multi-lane traffic, the aforementioned static methods fall short of the trajectory feasibility and security. Besides the right-of-way conflict between autonomous and human-driven vehicles, there exist significant differences in driving styles among human drivers also with driving emotions changing over time, which urges the automatic LC system to behave more cautious and flexible (Zhang et al., 2022a). In Li et al. (2022b) and Chhabra et al. (2023), the possible anger and unsafe behavior of human vehicles (HV) caused by autonomous vehicles (AV) were learned and analyzed. It is noteworthy that even the optimal LC trajectory proposed based on the original traffic scenario may become high-risk under the acceleration and preemption behavior of human drivers. To cope with this special scenario, some research has been put forward in a prudent and compromising manner. Li et al. established a decision-making model during the LC process to determine the environmental risks in real time (Li et al., 2022c). Once receiving the judgment of risk, the trajectory planning module would make the vehicle return to the original lane at four-time nodes. Yu et al. proposed an automatic LC system involving multiple decisions, one of which was returning to the original lane if discovering hazards and restarting the LC after no hazards (Yu et al., 2023). Fukuyama used game theory to judge the suitability of LC (Fukuyama, 2020). In most studies, intelligent vehicles must stop LC and return, but this may not be the optimal solution analogous to the scenario depicted in Fig. 1. Since the vehicle still has the ability to complete the LC. Fig. 1 shows that the black vehicle (HV) is offended by the red vehicle (AV) for the LC trend, and decides to speed up in order to reduce the distance from the front vehicle. In particular, by providing that the blue vehicle (HV) does not exhibit anti-congestion intent like the black vehicle (HV), a safer and more efficient method would be to transfer the LC target point from before the black vehicle to between the blue and the black. Zhang et al. shared similar ideas in their works (Zhang et al., 2021). They attempted to insist on LC and avoid vehicle-to-vehicle collisions by virtue of a small range of velocity and trajectory adjustments using the QP method. Nonetheless, the adjustments were decided based on a fixed safety distance without showing the dynamical characteristics of vehicle interpenetration gaps. For this reason, this work would like to present a real-time trajectory re-planning method for LC tasks to prevent the premature termination, achieving the LC goal as soon as possible while ensuring reasonable performance.

Compared to the original trajectory planning with a long preparation time, the re-planning function during the LC process requires a faster calculation and better real-time performance. Real time performance in the field of vehicles is an essential research field (Pan et al., 2019). Therefore, this work adopts the neural network model based on big data fitting to enhance the re-planning efficiency. To date, multiple studies in the field of vehicle autonomy have successfully employed data fitting models for the improvement of computational efficiency. Using the method of Deep Neural Networks (DNN), Nie et al. established a precise and efficient vehicle model of longitudinal-lateral dynamics (Nie et al., 2022; Pan et al., 2021). Keuntaek et al. applied the Inverse Reinforcement Learning (IRL) to quickly calculate the cost map for MPC (Lee et al., 2022). For the finite element analysis of the mechanical structure of electric vehicle battery packs, Zhang et al. proposed a DNN-based approach to achieve rapid performance prediction (Zhang et al., 2023; Pan et al., 2022). Rhode et al. presented a power prediction method for electric vehicles using a data-driven model that was constructed entirely with the available data collected from onboard sensors (Rhode et al., 2020).

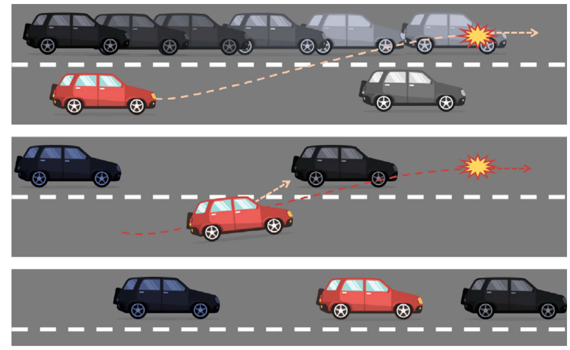

Fig. 1. The scenarios where re-planning are better than returning to the original lane.

This work proposes a real-time trajectory re-planning method for the conflicting formal strategies of Human Vehicle bursts during LC. The main innovations of this work are as follows:

- An analysis is conducted on the circumstances where intelligent vehicles may keep LC by trajectory modifying.
- Data-driven module has been developed through the use of two neural networks and a rule-based judgment method.
- Data experiments indicate that the trajectory re-planning approach can maintain safety.

The remainder of this paper is organized as follows: Section 2 gives the detailed introduction of a conventional trajectory planning method based on the quintic polynomial. In Section 3, a conflicting traffic scenario was established and the impact of several factors was analyzed. Section 4 describes the method for proposing new trajectories. Section 5 validates the proposed approach based on various numerical scenarios. Finally, this work is summarized.

2. Automated lane-changing model

2.1. Trajectory planning

Firstly, to realize the re-planning of LC trajectories, the basic algorithm of trajectory planning must be described in detail. A quintic polynomial was selected to describe the LC trajectory. It can satisfy basic principles in a simple LC scenario shown in Fig. 2 as:

$$\begin{cases} x(t) = a_0 + a_1 t + a_2 t^2 + a_3 t^3 + a_4 t^4 + a_5 t^5 \\ y(t) = b_0 + b_1 t + b_2 t^2 + b_3 t^3 + b_4 t^4 + b_5 t^5 \end{cases} \quad (1)$$

where a_i, b_i, $i = 0, 1, \ldots, 5$ are undetermined coefficients. Velocity and acceleration equations for a vehicle following the quintic trajectory are obtained by using the first and second derivatives of Eq. (1) as:

$$\begin{cases} \dot{x}(t) = a_1 + 2a_2 t + 3a_3 t^2 + 4a_4 t^3 + 5a_5 t^4 \\ \dot{y}(t) = b_1 + 2b_2 t + 3b_3 t^2 + 4b_4 t^3 + 5b_5 t^4 \end{cases} \tag{2}$$

$$\begin{cases} \ddot{x}(t) = 2a_2 + 6a_3 t + 12a_4 t^2 + 20a_5 t^3 \\ \ddot{y}(t) = 2b_2 + 6b_3 t + 12b_4 t^2 + 20b_5 t^3 \end{cases} \tag{3}$$

At the moment when the vehicle initiates a LC, the position of the vehicle is considered as the coordinate origin. The road direction is longitudinal, and the LC direction is lateral. The boundary conditions of the LC including the initial and final states of the LC trajectory are given by:

$$\begin{cases} x(0) = 0, \dot{x}(0) = vx_s, \ddot{x}(0) = ax_s \\ y(0) = 0, \dot{y}(0) = vy_s, \ddot{y}(0) = ay_s \end{cases} \tag{4}$$

$$\begin{cases} x\left(t_p\right) = x_p, \dot{x}\left(t_p\right) = vx_p, \ddot{x}\left(t_p\right) = ax_p \\ y\left(t_p\right) = y_p, \dot{y}\left(t_p\right) = vy_p, \ddot{y}\left(t_p\right) = ay_p \end{cases} \tag{5}$$

Assuming that the values in Eqs. (4) and (5) are known values, the coefficients of the quintic polynomial can be calculated using the following equation:

$$\begin{bmatrix} a_0 \\ a_1 \\ a_2 \\ a_3 \\ a_4 \\ a_5 \end{bmatrix} = T^{-1} \begin{bmatrix} x(0) \\ \dot{x}(0) \\ \ddot{x}(0) \\ x(t_p) \\ \dot{x}(t_p) \\ \ddot{x}(t_p) \end{bmatrix} \tag{6}$$

$$\begin{bmatrix} b_0 \\ b_1 \\ b_2 \\ b_3 \\ b_4 \\ b_5 \end{bmatrix} = T^{-1} \begin{bmatrix} y(0) \\ \dot{y}(0) \\ \ddot{y}(0) \\ y(t_p) \\ \dot{y}(t_p) \\ \ddot{y}(t_p) \end{bmatrix} \tag{7}$$

where T is a 6-junction matrix related to the time t_p:

$$T = \begin{bmatrix} 1 & 0 & 0 & 0 & 0 & 0 \\ 0 & 1 & 0 & 0 & 0 & 0 \\ 0 & 0 & 2 & 0 & 0 & 0 \\ 1 & t_p & t_p^2 & t_p^3 & t_p^4 & t_p^5 \\ 0 & 1 & 2t_p & 3t_p^2 & 4t_p^3 & 5t_p^4 \\ 0 & 0 & 2 & 6t_p & 12t_p^2 & 20t_p^3 \end{bmatrix} \tag{8}$$

It can be seen that after determining a total of 13 parameter values, including the 6 starting point parameters of Eq. (4), the 6 key parameters of Eq. (5), and the LC time of Eq. (8), the LC trajectory will be uniquely determined. The vehicle state at the beginning of LC is a known value, so x_0, $\dot{x}(0)$, $\ddot{x}(0)$, y_0, $\dot{y}(0)$, $\ddot{y}(0)$ are known values. In general, the target state of vehicle LC behavior in the lateral direction is also a fixed value, y_0 = lane width, $\dot{y}(0)$ and $\ddot{y}(0)$ are approximately 0. In the longitudinal direction, LC is essentially a queue-jumping behavior, and the end velocity and acceleration of LC are related to the average velocity and acceleration of the target lane's fleet. Therefore, based on the above analysis, 11 of the 13 parameters are fixed. Therefore, most studies based on quintic polynomials focus on the change of vehicle LC trajectory with LC time t_p and longitudinal displacement x_p, and seek the optimal solution within a certain range of values. The polynomial curve methodology has been proven to yield favorable results in various coordinate systems, including the geodetic coordinate system on which this study is based. In reality, the Frenet coordinate system (l-s) demonstrates impressive performance when dealing with curved roads. The main focus of this article is the establishment of a trajectory re-planning method. Consequently, the relationship between the Frenet coordinate system and the geodetic coordinate system, as well as the road curvature, were not considered. However, when dealing with curved roads, the application of this method can be effectively adapted through coordinate system transformation.

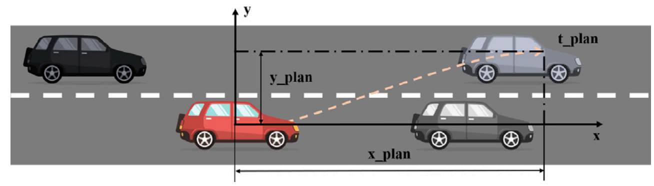

Fig. 2. Coordinate system for research on vehicle lane-changing behavior.

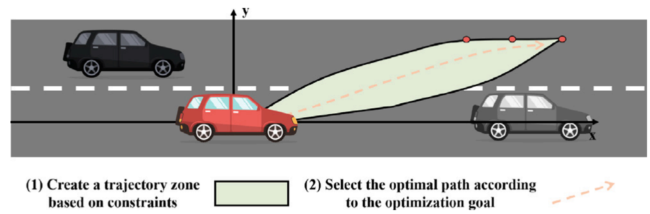

Fig. 3. Optimal trajectory optimization based on trajectory zone generation.

2.2. Trajectory zone generation

To design an optimal LC trajectory within a certain range of LC time t_p and longitudinal displacement x_p, two conditions: limitations, and optimization objectives, need to be considered. Limitations are the basic conditions that must be met in vehicle trajectory design. By limiting, a trajectory zone can be first created, which is called the trajectory zone, as shown in Fig. 3.

The generation of the trajectory zone is mainly determined by some limitations: position, time, velocity, comfort & stability, collision avoidance. Their mathematical formula is shown in Eq. (9). The vehicle's LC time and longitudinal distance should be controlled within a certain range. If the value is too large, it will lead to long-term driving between lanes and damage to traffic order; If the value is too small, it will cause the vehicle to have an excessive sense of LC, resulting in reduced driving comfort and even lateral instability. Therefore, it is necessary to limit the values of the two parameters to a certain range based on experience. Even though vehicles often need to undergo drastic acceleration and deceleration during LC, generally speaking, vehicles should not have behaviors such as parking, reversing, and exceeding the road velocity limit. Therefore, the driving velocity of the vehicle during LC also needs to be limited by upper and lower boundaries. Acceleration and jerk can often accurately reflect the comfort and stability of a vehicle during driving. In the vehicle body coordinate system, the lateral acceleration of the vehicle should not exceed 0.4 g, otherwise, it will lead to lateral instability of the vehicle. The longitudinal acceleration of the vehicle should not be too large, resulting in increased carsickness among passengers. Collision avoidance is the core of the trajectory zone. The prediction of safety status requires accurate environmental awareness, environmental vehicle trajectory prediction, and safety judgment models. Generally speaking, during the LC process, three vehicles are mainly concerned, as shown in Fig. 4, including the forward vehicles in the current lane and the front and rear vehicles in the target lane.

$$\begin{aligned} & x_{min} < x(t) < x_{max} \\ & y_{min} < y(t) < y_{max} \\ & v_{x,min} < v_x(t) < v_{x,max} \\ & \left|a_x(t)\right| < a_{x,max} \\ & \left|a_y(t)\right| < a_{y,max} \\ & \left|j_x(t)\right| < j_{x,max} \\ & \left|j_y(t)\right| < j_{y,max} \end{aligned} \tag{9}$$

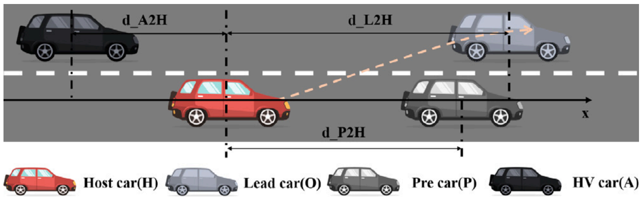

Fig. 4. Environmental vehicles that may collide during lane changes.

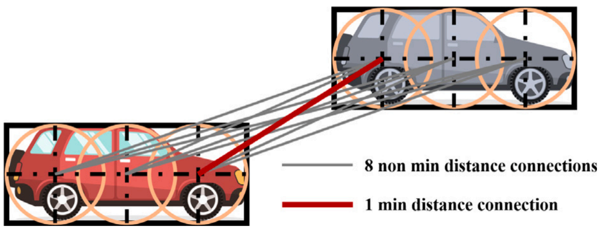

Fig. 5. A three-circle model for accurately judging the collision state.

In the design of the trajectory planning module, it is generally believed that the perception module and the prediction module have provided reliable information for it, and will not design functions separately in the trajectory planning module. In safety judgment models, common methods include safety distance, artificial potential field, risk evaluation indicators, and so on. The safety distance is the simplest and most reliable calculation model. However, in the safety judgment in this work, the vehicle is not a simple particle, with a rectangular geometric shape of approximately 1.8 ∗ 3.8 m. At this time, if the relative distance between the particles of two vehicles is judged, a problem may arise. If the collision value is taken as 1.8 m, it will lead to potential collisions. If the collision value is taken as 3.8 m, it may lead to significant lateral vacancy generation and is not conducive to a reasonable location selection. To solve this problem of safety distance determination, a common approach is to use a three-circle model to ensure computational efficiency while improving the accuracy of collision determination (Bae et al., 2022), as shown in Fig. 5.

After determining a trajectory, it is necessary to deduce the minimum distance between the vehicle and the environmental vehicle in the future. If the main vehicle and the environment vehicle always maintain a certain safety distance during the traversal of all time nodes, the safety conditions are met. These four constraints set the lowest feasible criteria for trajectory planning, and all values that meet these conditions constitute the trajectory zone. The values given by Ding et al. (2021) are used. The trajectory zone is obtained and shown in Fig. 6. It should be noted that they do not distinguish between the road coordinate system and the vehicle coordinate system in terms of acceleration limits, which is unreasonable. Therefore, this issue has been corrected in the calculation process in this work. The main parameter selection is shown in Table 1. In this paper, H represents the controlled vehicle, and L represents the leading vehicle in the original lane. O, A, and B are vehicles in the H target lane, and their positional relationships are shown in Figs. 4 and 8.

2.3. Optimal trajectory generation

All values in the trajectory zone can provide a standard vehicle LC trajectory, but there are still considerable differences between different trajectories. At this point, some evaluation functions can be proposed to analyze the advantages and disadvantages among trajectories. However, it should be emphasized that there are significant differences in the evaluation functions of different scholars. The selection of coefficients for different performances is often subjective, and this work only provides a common evaluation function that considers five factors as a reference.

$$\min J\left(t_p, x_p\right) = w_1 W_1 + w_2 W_2 + w_3 W_3 + w_4 W_4 + w_5 W_5 \\ = w_1 \frac{\int_0^{t_p} j_x^2(t)dt}{j_{x,\max} a_{x,\max}} + w_2 \frac{\int_0^{t_p} j_y^2(t)dt}{j_{y,\max} a_{y,\max}} + w_3 \frac{x_p}{w} + w_4 \dot{f}_v + w_5 (d_{min} - 2r_v) \tag{10}$$

where W_1 and W_2 represent comfort indicators; W_3 is the LC efficiency index, w is the lane width; W_4 is the fuel economy index, and its equation is $\dot{f}_{accel} = a(t)\left(r_0 + r_1 \cdot v(t) + r_2 \cdot v^2(t)\right)$ on the trajectory with velocity changes. r_0, r_1 and r_2 are the correlation coefficient of fuel consumption.; W_5 is a safety index, d_{min} is the estimated minimum vehicle distance for the entire LC trajectory, and r_v is the radius of the minimum unit circle for the three-wheel model. w_i (i = 1, 2, …, 5) is the weight coefficient. The five factors are adjusted to the consistent importance through the normalization method. In reality, the coefficient values employed in this optimization function are subjective in nature. When developers prioritize the vehicle's comfort, they tend to amplify the values of w1 and w2. Similarly, if additional safety is given more emphasis, the value of w3 can increase in a similar manner. The weightage given to fuel consumption is represented by w4, while the significance attributed to lane change efficiency is denoted by w5. The determination of these values is often intentional and necessitates substantial fine-tuning. This work simplifies their treatment by assigning them identical numerical representations, implying their equal importance. This approach is a simplification. However, if there are additional requirements, these parameters can be further fine-tuned to accomplish multi-objective optimization.

The method of traversing is used to find the global optimal solution and obtains the optimal LC curve (2.8 s, 86.5 m) under the working condition in Fig. 6. In a 5-point evaluation, the lowest LC cost is 1.7908. The lower the cost J, the more satisfactory the trajectory is. The trajectory scatter diagram of the optimal trajectory is shown in Fig. 7. It can be seen that the planned trajectory is smooth and maintains a certain relative distance from the environment vehicles.

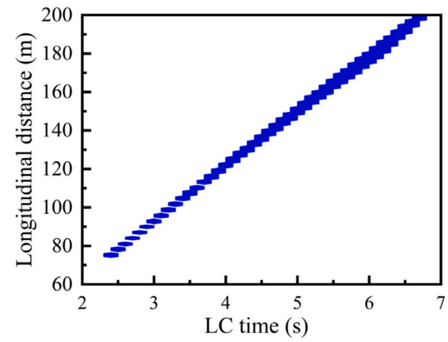

Fig. 6. Range of lane-changing trajectory zone.

Table 1
Limitations on trajectory zone generation.

Parameter	Value	Unit
H initial velocity	30	m/s
A&O velocity	33.3	m/s
P velocity	28.8	m/s
Longitudinal displacement	60–200	m
LC time	2–8	s
H-P&O longitudinal distance	5	m
H-A longitudinal distance	30	m
lane width	3.75	m
Max acceleration	0.4	g
Max velocity	40	m/s
Max velocity	0	m/s
Safe distance	0.4	m
Vehicle length and width	3.8 ∗ 1.8	m ∗ m

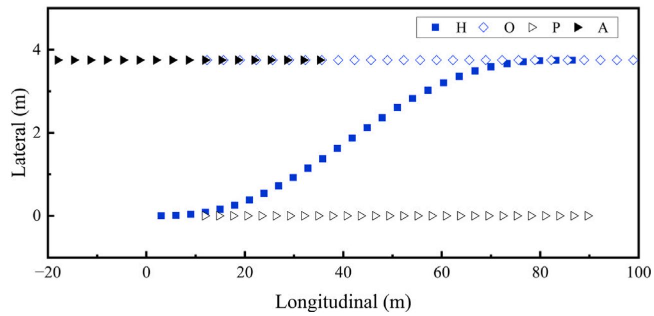

Fig. 7. Optimal trajectory design with the cost function J.

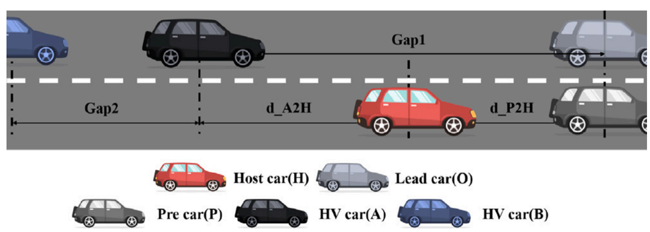

Fig. 8. A general scenario for analyzing LC trajectory replanning.

Table 2
Numerical differences between two environments.

Parameter	Value (highway)	Value (city)	Unit
H initial velocity	30	12	m/s
B&A&O velocity	33.3	15	m/s
P velocity	28.8	12	m/s
Max additional LC time	4	4	s
H-P longitudinal distance	9	9	m
H-O longitudinal distance	9	9	m
H-A longitudinal distance	−24	−34	m
H-B longitudinal distance	−38	−58	m
lane width	3.75	3.75	m
Vehicle length and width	4 ∗ 1.8	4 ∗ 1.8	m ∗ m

3. Conflicting traffic model

As mentioned in the Intro chapter, human drivers can speed up recklessly because of dissatisfaction with the lane insertion behavior of other vehicles. At the risk of these dangerous vehicles, reasonable trajectory re-planning must be attempted. But it is impossible to achieve skilled re-planning of the LC trajectory in all scenarios within the trajectory zone that meet the constraints. The goal of this chapter is to explore the conditions under which vehicles can achieve qualified trajectory re-planning based on different influencing factors. In order to do this, it is first necessary to propose a few typical traffic scenarios that can be used for analysis. The main contributions of this work are two different LC scenarios, representing cities and highways respectively. In both scenarios, the traffic flow structure is the same, as illustrated in Fig. 8. However, there are significant differences in the parameters between the two, as shown in Table 2.

In urban traffic scenarios, the smaller the vehicle spacing, the lower the average velocity, the larger the average longitudinal distance for LC, and the harder the LC behavior. In this scenario, follow the method described in the previous chapter to find the trajectory zone and obtain a total of 980 sets of feasible trajectories. Among all tracks, two sets of tracks were selected for subsequent analysis: The first group is the optimal LC trajectory, 70.5 m to 5.3 s, with the lowest LC cost of 0.7526. The second group is a longer LC trajectory, 108 m to 8.1 s, with a LC cost of 1.1183. Correspondingly, in highway traffic scenarios, the average velocity is higher and LC is more difficult. Under the mandatory safety requirement of 0.4 m, a total of 76 feasible trajectories were obtained. Among all tracks, two sets of tracks were selected for subsequent analysis: The first group is the optimal LC trajectory, 86.5 m to 2.8 s, with the lowest LC cost of 1.7908. The second group is a longer LC trajectory, 181 m to 6.2 s, with a LC cost of 3.1006. Based on the above analysis, the following will analyze each of the different factors that may affect the feasibility of adhering to LC behavior. In this work, four factors were selected for specific analysis: original LC trajectory, risk triggering time, HV conflict performance, and acceleration vehicle queue. In order to better illustrate the 10 cases proposed in this chapter, the Table 3 summarizes the parameters.

3.1. Original trajectory

Firstly, this chapter analyzes whether the selection of the original trajectory will affect the difficulty of trajectory re-planning. To better control variables, each study of a single variable will implement a description of the current values of other fixed variables. Cases 1, 2, 3, and 4 are comparative cases that use the original trajectory as a differentiation design. Case 1 & 2 use an urban traffic environment, with a trigger time of 1.1 s, a safety distance of 2.2 m, and a conflict vehicle A with an acceleration of 1.5 m/s^2. It should be noted that the trigger time represents the time point at which the vehicle detects a safety risk. Under the same conditions, they analyze the feasibility differences of trajectory re-planning for two different original urban LC trajectories. Case 1 uses a short distance trajectory (70.5 m, 5.3 s) in an urban environment, and its re-planned trajectory zone is shown in Fig. 9(a). The comparison between the original trajectory and the optimal re-planned trajectory is shown in Fig. 9(b). At 1.1 s, vehicle H began to re-plan the trajectory due to the detection of significant acceleration behavior in vehicle A. The trajectory parameters obtained are (59 m, 1.1 + 3.2 s). It can be seen that the vehicle has chosen to accelerate and change lanes in advance, considering that although Vehicle A accelerates vigorously, there is a large gap in its original position. When additional attention is needed, the trajectory zone itself is extremely small in the current situation. Case 2 uses a long-distance trajectory (108 m, 8.1 s) in an urban environment, and its re-planned trajectory zone is shown in Fig. 10(a). The comparison between the original trajectory and the optimal re-planned trajectory is shown in Fig. 10(b). The trajectory parameters obtained are (121 m, 1.1 + 10.2 s). As can be seen, Case 2 chose to extend the LC time after considering the conflicting intentions of Vehicle A, and allowed Vehicle A to accelerate first and then follow. Compared to Case 1, its trajectory zone is larger. This means that vehicles can re-plan more LC trajectories. At this point, it is easier to achieve the vehicle's trajectory re-planning.

Case 3 & 4 use a highway traffic environment, with a trigger time of 1.1 s, a safety distance of 2.2 m, and a conflict vehicle A with an acceleration of 4.0 m/s^2. Under the same conditions, Case 1 and Case 2 analyze the feasibility differences of trajectory re-planning for two different original urban LC trajectories. Case 3 uses a short-distance trajectory (86.5 m, 2.8 s) in a highway environment, and its re-planned trajectory zone is shown in Fig. 11(a). The comparison between the original trajectory and the optimal re-planned trajectory is shown in Fig. 11(b) The trajectory parameters obtained are (90 m, 1.1 + 2.9 s). It can be seen that the degree of danger in Case 3 is relatively low, and a safe trajectory can be reasonably planned as long as the target location is appropriately fine-tuned. Similar to Case 1, the trajectory zone available for trajectory adjustment in the current situation is very small. Case 4 uses a long-distance trajectory (181 m, 6.2 s) in a highway environment, and its re-planned trajectory zone is shown in Fig. 12(a). The comparison between the original trajectory and the optimal re-planned trajectory is shown in Fig. 12(b). The trajectory parameters obtained are (242 m, 1.1 + 8.7 s). Similar to Case 2, Case 4 is also a strategy of letting Car A go first.

From the above four cases, it can be seen that: in the case of short LC times and relatively large rear-side oncoming distances, even if the vehicle has conflicting intentions, based on the predetermined

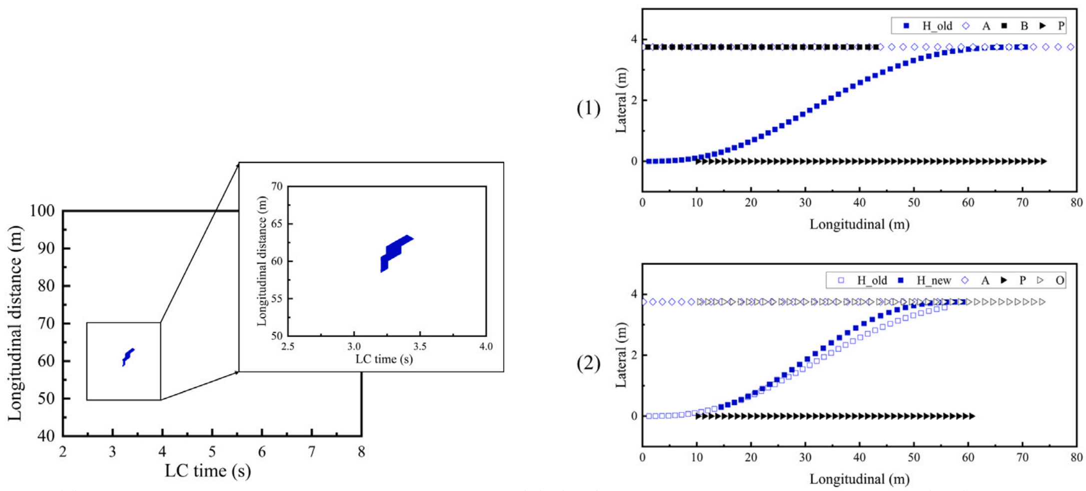

(a) Re-planning trajectory zone analysis

(b) (b-1) the original planning trajectory (b-2) comparison between the original planning trajectory and the optimal re-planning trajectory

Fig. 9. Feasibility analysis of trajectory re-planning in Case 1.

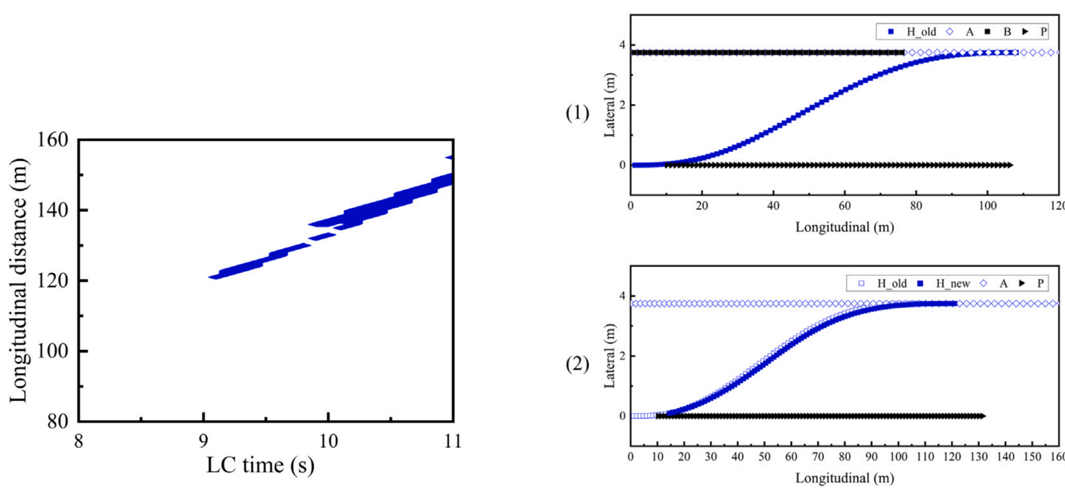

(a) Re-planning trajectory zone analysis

(b) (b-1) the original planning trajectory (b-2) comparison between the original planning trajectory and the optimal re-planning trajectory

Fig. 10. Feasibility analysis of trajectory re-planning in Case 2.

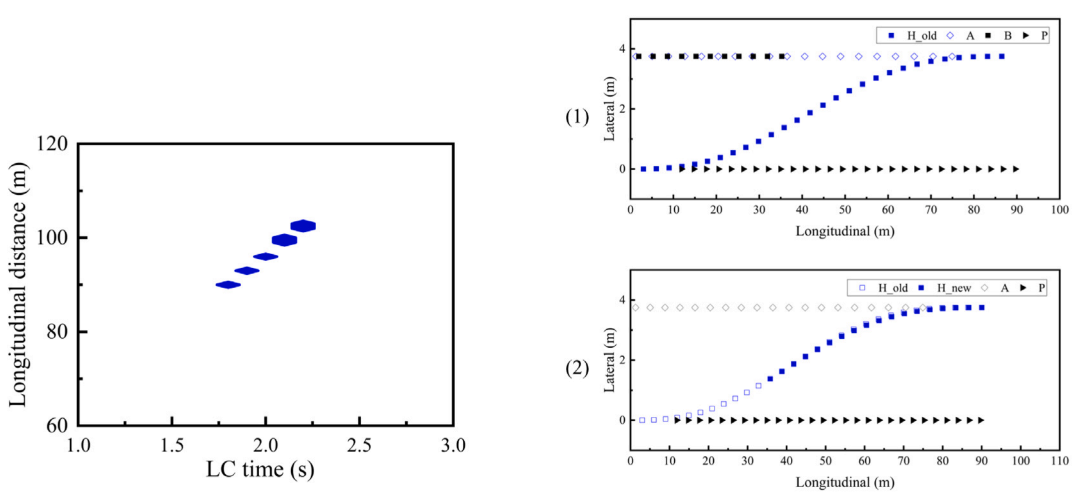

(a) Re-planning trajectory zone analysis

(b) (b-1) the original planning trajectory (b-2) comparison between the original planning trajectory and the optimal re-planning trajectory

Fig. 11. Feasibility analysis of trajectory re-planning in Case 3.

Table 3
Values of 10 cases with four factors.

Case	Key feature	Road	Original trajectory	Trigger time	Acceleration
1	Original trajectory	City	70.5 m, 5.3 s	1.1 s	1.5 m/s^2
2	Original trajectory	City	108 m, 8.1 s	1.1 s	1.5 m/s^2
3	Original trajectory	Highway	86.5 m, 2.8 s	1.1 s	4 m/s^2
4	Original trajectory	Highway	181 m. 6.2 s	1.1 s	4 m/s^2
5	Trigger time	City	108 m, 8.1 s	–	1.5 m/s^2
6	Trigger time	Highway	181 m. 6.2 s	–	4 m/s^2
7	HV acceleration	City	108 m, 8.1 s	1.1 s	–
8	HV acceleration	Highway	181 m. 6.2 s	1.1 s	–
9	Multiple conflict HV	City	108 m, 8.1 s	–	1.5 m/s^2
10	Multiple conflict HV	Highway	181 m. 6.2 s	–	4 m/s^2

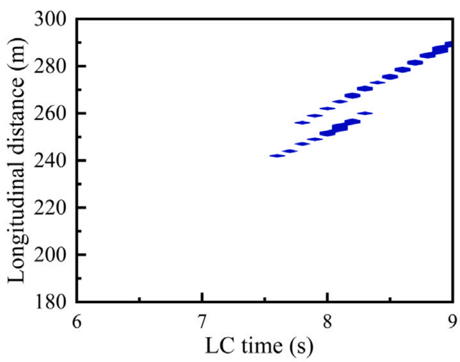

(a) Re-planning trajectory zone analysis

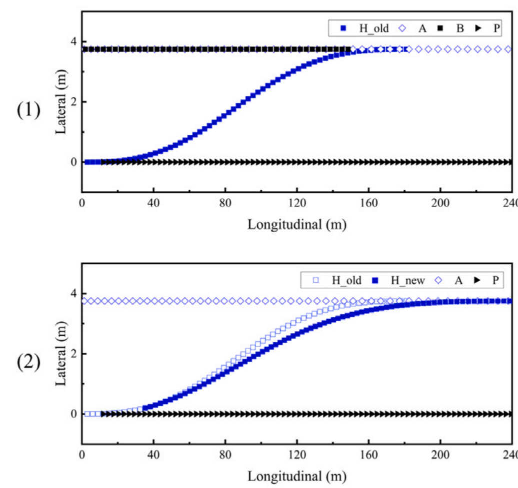

(b) (b-1) the original planning trajectory (b-2) comparison between the original planning trajectory and the optimal re-planning trajectory

Fig. 12. Feasibility analysis of trajectory re-planning in Case 4.

safety state, the optimal choice for the vehicle is still to accelerate and select an empty gap in front of the vehicle. Taking Case 1 and Case 3 as examples, vehicles only need to increase their driving speed appropriately to achieve rapid LC. Complete the LC behavior before vehicle A accelerates. However, it is also found that accelerating based on the original trajectory is a dangerous behavior. At this point, the area of the vehicle trajectory zone will become very small due to velocity and acceleration limitations. This indicates that accelerating and persisting in overtaking during LC is reasonable but also difficult to achieve.

In contrast, observe Case 2 and Case 4, both of which are original trajectory planning for a long time. In this context, when vehicles face severe safety tests, they are more willing to avoid risks by extending the LC time and longitudinal distance. This deceleration trajectory re-planning is more consistent with the definition of safety, so the area of its trajectory zone will be significantly larger than Case 1 and Case 3. This indicates that when the LC trajectory of the vehicle itself is relatively slow, it is often possible to flexibly respond to risks through deceleration.

* Summary 1: For a relatively rapid lane-changing trajectory, the lane-changing strategy for vehicle re-planning in the face of danger is often to accelerate and complete the lane-changing first. The faster the lane-changing behavior, the more difficult it is to deal with potential safety hazards that occur during the lane-changing process. At this point, the feasibility of lane-changing trajectory re-planning is relatively low. Conversely, the slower the lane-changing, the easier it is to deal with potential safety hazards that occur during the lane-changing process. It is easier for vehicles to safely and smoothly re-plan their lane-changing trajectory by slowing down.

3.2. Replanning trigger time

Case 5 uses a long-distance original trajectory (108 m, 8.1 s) in an urban environment, with a conflict vehicle A with an acceleration of 1.5 m/s^2. Under these conditions, Case 5 (also 6) analyzes the change in the area of the re-planned trajectory zone with trigger time in the urban environment. As shown in Fig. 13, as the vehicle's safety risk detection time lags, the number of samples in the re-planned trajectory zone rapidly decreases. At 1.2 s, the vehicle could no longer plan a safe and effective LC route. Case 6 uses a long-distance original trajectory (181 m, 6.2 s) in a highway environment, with a conflict vehicle A with an acceleration of 4.0 m/s^2. As shown in Fig. 13, as the trigger time increases, the number of available rescheduled trajectories decreases rapidly. This is very similar to Case 5.

According to Case 5 and Case 6, the later a vehicle initiates a LC behavior, the more obvious the area of the available LC trajectory zone will also be reduced. When the vehicle has already undergone significant lateral road movement (both cases 5 and 6 have a maximum decision time of 1.2 s), the vehicle is no longer able to re-plan a reasonable optimal lane-changing trajectory using the quintic polynomial programming method. Therefore, vehicle environmental awareness and risk judgment should be made as early as possible.

* Summary 2: With the increase of the trigger time for vehicles to sense road risks, the feasibility of route re-planning decreases rapidly.

3.3. HV conflict performance

Case 7 uses a long-distance original trajectory (108 m, 8.1 s) in an urban environment, with a trigger time of 1.1 s, and a safety distance

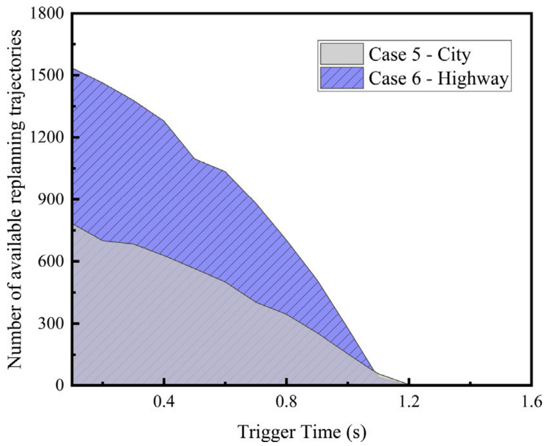

Fig. 13. Changes in the number of available reprogramming trajectories over decision time in urban environments.

of 2.2 m. Under these conditions, Case 7 (also 8) analyzes the change of the area of the re-planned trajectory zone with collision behavior's acceleration of HV in the urban environment. Specifically, the closer the acceleration of A approaches a moderate value, the fewer tracks available for re-planning. The histogram shows the shape of a valley. Case 8 uses a long-distance original trajectory (181 m, 6.2 s) in a highway environment, with a trigger time of 1.1 s, and a safety distance of 2.2 m. Fig. 8 also shows a similar valley shape.

According to Case 7 and Case 8, the acceleration of conflicting HV will have a significant impact on the likelihood of LC re-planning. If the acceleration is too small, the LC position of the vehicle is always in front of the accelerating vehicle. The vehicle can avoid the safety risk of HV by accelerating. If the acceleration is excessive, the LC position of the vehicle is always behind the accelerating vehicle. The vehicle can avoid the safety risk of HV by decelerating. Therefore, when the acceleration of a conflicting vehicle just collides with the LC position of the current vehicle, it is difficult to re-plan the LC trajectory of the vehicle. Therefore, when the acceleration of conflicting vehicles is large or small enough, the re-planning of the trajectory is feasible. On the contrary, the opportune acceleration can lead to dangerous traffic scenarios and impossible LC trajectory re-planning.

It should be added that the valley shapes in Figs. 14(a) and 14(b), the number of feasible trajectory reprogramming samples for accelerated LC behavior is smaller than that for deceleration LC behavior. This also laterally confirms the viewpoint proposed in Summary 1.

* Summary 3: In the face of conflicting vehicles, there are two feasible solutions: accelerating early lane-changing behavior and decelerating delayed lane-changing behavior. When the acceleration of conflicting vehicles is large, the optimal trajectory re-planning scheme is to slow down and wait for them to pass. On the contrary, the optimal trajectory re-planning scheme is to accelerate early passage. However, when the conflicting vehicle has a moderate acceleration, the vehicle cannot find a reasonable re-planning trajectory in the range of trajectory zone values.

3.4. Multiple conflict HV

Case 9 uses a long-distance original trajectory (108 m, 8.1 s) in an urban environment, with a trigger time of 1.1 s, and a safety distance of 2.2 m. Case 10 uses a long-distance original trajectory (181 m, 6.2 s) in a highway environment, with a trigger time of 1.1 s, and a safety distance of 2.2 m. The variable is the magnitude of acceleration. In particular, vehicle A is followed by vehicle B which maintains the same acceleration behavior as A. As shown in Fig. 15, when there is a follow-up with similar acceleration behind a conflicting vehicle, the current vehicle cannot redesign a LC trajectory by slowing down within the available search range. Therefore, Fig. 15 is more like a truncated version of Figs. 14(a) and 14(b). It should be emphasized that in Fig. 15, it can be seen that in Case 9, there is still a possibility of persisting in LC when the acceleration is close to 3 m/s^2. However, compared to Fig. 14(b), Case 10 cannot achieve LC in acceleration scenarios above 3 m/s^2. So there is no display of situations above 3 m/s^2 here.

Cases 9 and 10 are more realistic. In fact, in a traffic environment, vehicles in the lane often form a stable fleet structure. Assuming that following a conflicting vehicle always maintains similar traffic behavior to that of the vehicle in front, the LC behavior itself is more difficult. Therefore, the rear vehicle also shows a willingness not to be inserted into the team by the current vehicle. Compared to Cases 7 and 8, it can be seen that when the acceleration of the adjacent lane is low, the vehicle can still pass ahead of time by accelerating. However, if the acceleration of a conflicting vehicle is large, even if the vehicle wants to change lanes to the rear position of the conflicting vehicle through deceleration, the similar acceleration behavior of the rear vehicle does not allow the vehicle to be inserted into its gap. Therefore, the high acceleration of conflicting vehicles at this time will lead to the inability of the vehicle to re-plan the LC trajectory.

* Summary 4: When using deceleration as a lane-changing rescheduling scheme, it is not possible to complete the lane-changing trajectory rescheduling if the rear vehicles of conflicting vehicles exhibit similar anti-congestion behavior.

4. Real-time trajectory replanning method

To re-plan a safe LC trajectory, as shown in Fig. 16, three main parts need to be completed. Therefore, the logic of the main modules designed in this article is first explained. Then the specific description of the selected neural network model was provided.

4.1. Trajectory replanning logic

First of all, Determine whether the vehicle is likely to collide with high-risk vehicles in the environment. Vehicles need to re-plan their routes when they perceive the impact of the dangerous environment. If the autonomous vehicle does not perceive the emotions of other vehicles in the driving scene, it cannot judge the safety degree of the vehicle during driving. This is a very dangerous situation. Therefore, good environmental awareness parameters and risk assessment rules for real-time judgment are the basis for restarting vehicles for LC trajectory planning. This part should be judged by the vehicle prediction module, which is not the core point of this work. However, to cooperate with the following work, a simple vehicle safety judgment mechanism model was built. It is assumed that autonomous vehicles have a certain delay time in understanding the driving acceleration of HV in the environment. So when a vehicle suddenly experiences a temporary high acceleration after observing a vehicle running at a constant velocity for a long time, it is not possible to determine whether it is a temporary or long-term behavior of the vehicle. Therefore, the vehicle potential acceleration evaluation index for the vehicle is

$$a_{think} = a_{sudden} * \frac{t_{sudden}}{t_{sudden} + t_{delay}} \tag{11}$$

where, a_{think} refers to the estimated acceleration of autonomous vehicle to a vehicle in the environment, a_{sudden} refers to the average acceleration of the vehicle in a short time, t_{sudden} refers to the duration of sudden acceleration, and t_{delay} refers to the hysteresis of autonomous vehicle's judgment. Based on the estimated vehicle acceleration, the autonomous vehicle judges the impact of environmental vehicles on the whole process of LC, and determines whether to re-plan the driving trajectory. This equation can simply represent the risk response speed of AV in a dangerous scenario.

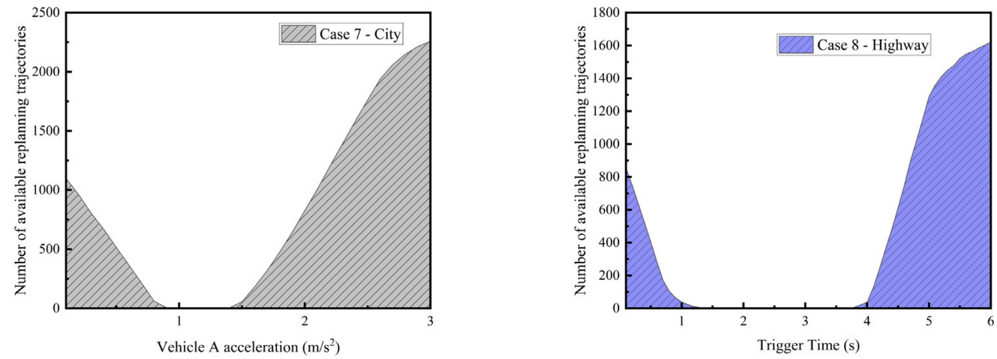

(a) Case 7 (b) Case 8

Fig. 14. Changes in the number of available reprogramming trajectories over vehicle A's acceleration in urban environments.

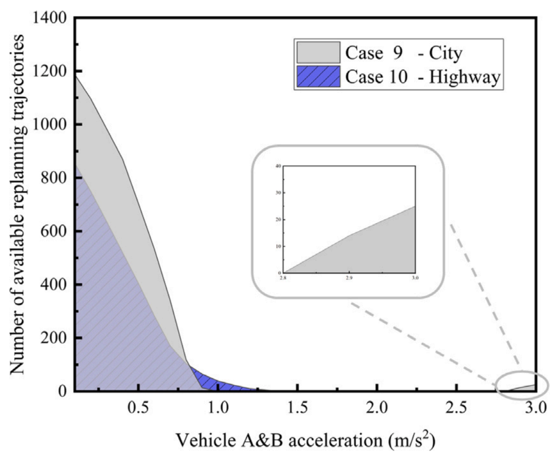

Fig. 15. Changes in the number of available reprogramming trajectories over vehicle A&B's acceleration in urban environments.

Then, determine whether there is a possibility for the vehicle to achieve standard trajectory re-planning. Finally, re-design the LC trajectory at the current time node, and try to meet the goal of local optimization. On the premise of clarifying the safety risks of the current vehicle due to acceleration in the target lane, the vehicle must first determine whether it is feasible to adhere to the lane-change behavior by adjusting the trajectory. Even a re-planned lane-change trajectory, should meet basic trajectory planning requirements also. Then, on the premise of existing trajectory planning and feasibility of LC, the vehicle uses the same quintic polynomial planning algorithm to re-plan its trajectory.

In fact, using the method of traversing all feasible values can solve the above two points simultaneously. Because of the range of values, all values are evaluated for feasibility and objective functions. Assume that the vehicle needs to find a possible re-planned LC trajectory under a matrix input of 125 ∗ 80 (i.e., 125 m value range, unit interval of 1 m. 8 s value range, unit interval of 0.1 s), and each specific x and t will determine safety by traversing the expected trajectory of 10 ∗ t for future lane-change. In finding whether there is a feasible trajectory zone and searching for the optimal trajectory, it can be seen that the traversal method is an extremely cumbersome and time-consuming method. However, at the same time, as shown in Fig. 13, the number of feasible LC trajectories decreases significantly with the passage of trigger time, so the real-time requirements for finding the optimal rescheduling LC trajectory are extremely high. Therefore, a method based on data fitting model was proposed to solve the real-time problem. For using data fitting model, the process of finding a LC trajectory and re-planning, LC process should be distinguished into two processes: the determination of the existence of trajectory zones and the acquisition of trajectory parameters. Dividing the process will better match the characteristics of the data fitting model, and the reasons will be explained in detail in the next section. After three processes, if a data fitting model is used, an additional safety verification behavior needs to be added. The reason for this will be explained in detail in Numerical Validation 1.

4.2. Data fitting model

Data fitting models are a hot research spot in recent years. Based on the idea of machine learning, complex data processing can be made computationally fast and almost real-time because the calculation burden mainly lies on the phase of offline training. Data fitting models can be divided into two categories based on the differences in their output: classifiers and regression fitters. The output of the classifier is fixed to several known values. For example, a vehicle lane-change decision model is a typical classifier whose operational outputs are left lane, right lane, and straight. The regression fitter outputs continuous values, such as the vehicle speed prediction module for autonomous vehicles. Its output is a specific vehicle speed value, not a gear classification of vehicle speed.

Following the previously mentioned design logic, the basic modules designed in this paper are shown in Fig. 17. The inputs to LC trajectory re-planning used in this work are environmental parameters, and the outputs are trajectory parameters: the LC time t and the longitudinal displacement x. We do not use the coefficients of the polynomial curves as outputs here because these coefficients are often very sensitive. Very small deviations can result in large changes in the curve. Therefore, the trajectory parameters were selected to be the output. With the help of Eq. (6) as well as Eq. (7), an appropriate polynomial curve may be obtained. While this may waste some computation time, it is a necessity. As the vehicle enters the LC process, the model first enters a waiting state. When the vehicle detects a hazard during LC, it immediately enters operational logic. This risk, as noted above, may stem from human drivers' awareness of lane occupancy, leading to unreasonable accelerating behavior of the HV.

The replanning LC trajectory should also be divided into two parts: the classification of the presence and absence of re-planned trajectory zones, and the re-planned trajectory's fitting after confirming the presence of trajectory zones. If a set of infeasible data is input into the LC trajectory re-planned model, an unreasonable set of trajectories will be obtained. This is a characteristic of data fitting models, which can only obtain the correct output for matching inputs. Therefore, dividing the LC trajectory into two parts: classifier and regression fitting, is not only the idea of the original lane-change trajectory planning method but also the necessary condition to ensure correct output. This work mainly uses the neural network (NN) method to build data-fitting models. NN

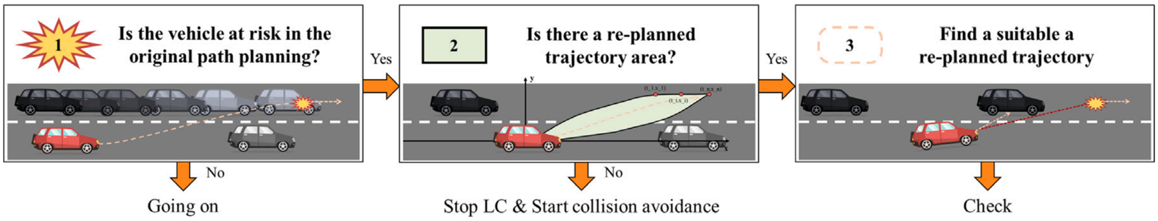

Fig. 16. Three main steps to achieve lane-changing in risk scenarios.

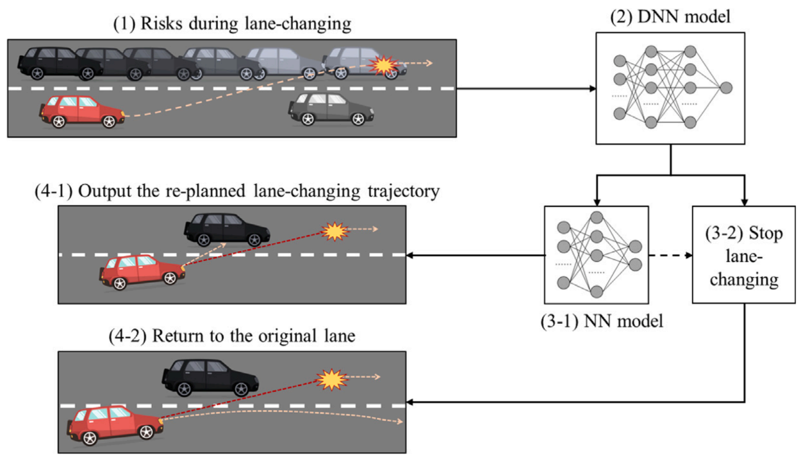

Fig. 17. Framework diagram of lane-changing trajectory re-planning module using two neural networks.

with multiple hidden layers strongly reflects the nonlinear relationship between input and output in theory. In most cases, NN is more suitable for high-dimensional data in complex scenes than algorithms such as support vector machine, K-nearest neighbor, and random forest. Generally, NN training can be divided into forward propagation and back propagation updates. The forward propagation algorithm should satisfy the equation to train the NN model:

$$\boldsymbol{X}^n = \sigma(\boldsymbol{Z}^n) = \sigma\left(\boldsymbol{W}^n \boldsymbol{X}^{n-1} + \boldsymbol{B}^n\right) \tag{12}$$

where $\boldsymbol{X}^n$ represents the output value vector of neurons at layer n, $\boldsymbol{B}^n$ represents the deviation matrix, and $\boldsymbol{W}^n$ represents the weight matrix from layer $n-1$ to layer n. During back propagation, the following equation is used to change the weight matrix and deviation matrix:

$$\boldsymbol{W}^n = \boldsymbol{W}^n - \alpha \frac{\partial \boldsymbol{L}}{\partial \boldsymbol{W}} \tag{13}$$

$$\boldsymbol{B}^n = \boldsymbol{B}^n - \alpha \frac{\partial \boldsymbol{L}}{\partial \boldsymbol{B}} \tag{14}$$

where α and L represent the learning rate and loss function, respectively. The loss function is continuously reduced by updating the weight and deviation matrices. In general, the accuracy of the NN model increases as the loss function decreases.

For the construction of the fundamental NN model, there are two key parameters: the number of hidden layers and the number of hidden layer neurons. First of all, regarding the selection of NN layers, there are such conclusions in the AI research field: For the matching relationship of conventional features (such as mathematical data and conventional signals), the setting of 1–2 fully connected hidden layers can effectively reflect the correlation features. However, for high-dimensional features such as images, it is often necessary to extract hidden features in the image for classification or regression with more than 3 layers of neurons. A large number of continuous digital features are used as input in this paper, which conforms to the hidden layer setting conditions of the NN. For the selection of the number of neurons in the hidden layer, there are usually three methods: empirical equation, recommended value range, and ergodic test. The study of empirical equations and the value range is often diverse, and even some studies still have contradictions. Therefore, the two methods for selecting the number of neurons can only be used as auxiliary values, and the selection of the optimal model still needs many attempts and comparisons. One empirical equation adopted is mathematically expressed as follows:

$$N_h = \frac{N_s}{j\left(N_x + N_y\right)} \tag{15}$$

where Ns represents the number of training samples, Nx and Ny represent the number of neurons in the input and output layers, respectively, and parameter j is a custom coefficient ranging from 2 to 10. According to this empirical equation, if about 20 features are used for this analysis, in the case of 5000 training samples, the reasonable value should be around 30. In the value range method, there are many regulations. One rule is that the number of neurons should be greater than the average of input neurons and output neurons, and less than the sum of input neurons and output neurons. Another one is the number of neurons shall be selected at two-thirds of the mean number of input neurons and output neurons, and shall not be less than one-third. They are widely used and therefore have some reference value.

For a total of 75 sets of original trajectories corresponding to 6 sets of current states of the vehicle and 10 sets of conflicting states The input parameters and the output of the trajectory area are different for each data set. This is achieved by splitting the data set into 90% of the training set and 10% of the test set. Two neural networks are employed in this work. In the case of the first neural network classifier, its input consists of three parameters: the original trajectory information, the judgment trigger time, and the risk vehicle information. The output is the question of whether there exists a feasible LC trajectory to continue the LC. Only yes and no are present in the output. As in our previous research on LC vehicle decision models, we used a DNN with two hidden layers to match this inconspicuous relation (Du et al., 2023). Ten neurons for each hidden layer were chosen. This choice of quantity is a locally optimal value obtained through experiment and small scale validation. The model has already performed well under this selection method. The accuracy of the DNN classifier is 99.6%, and the

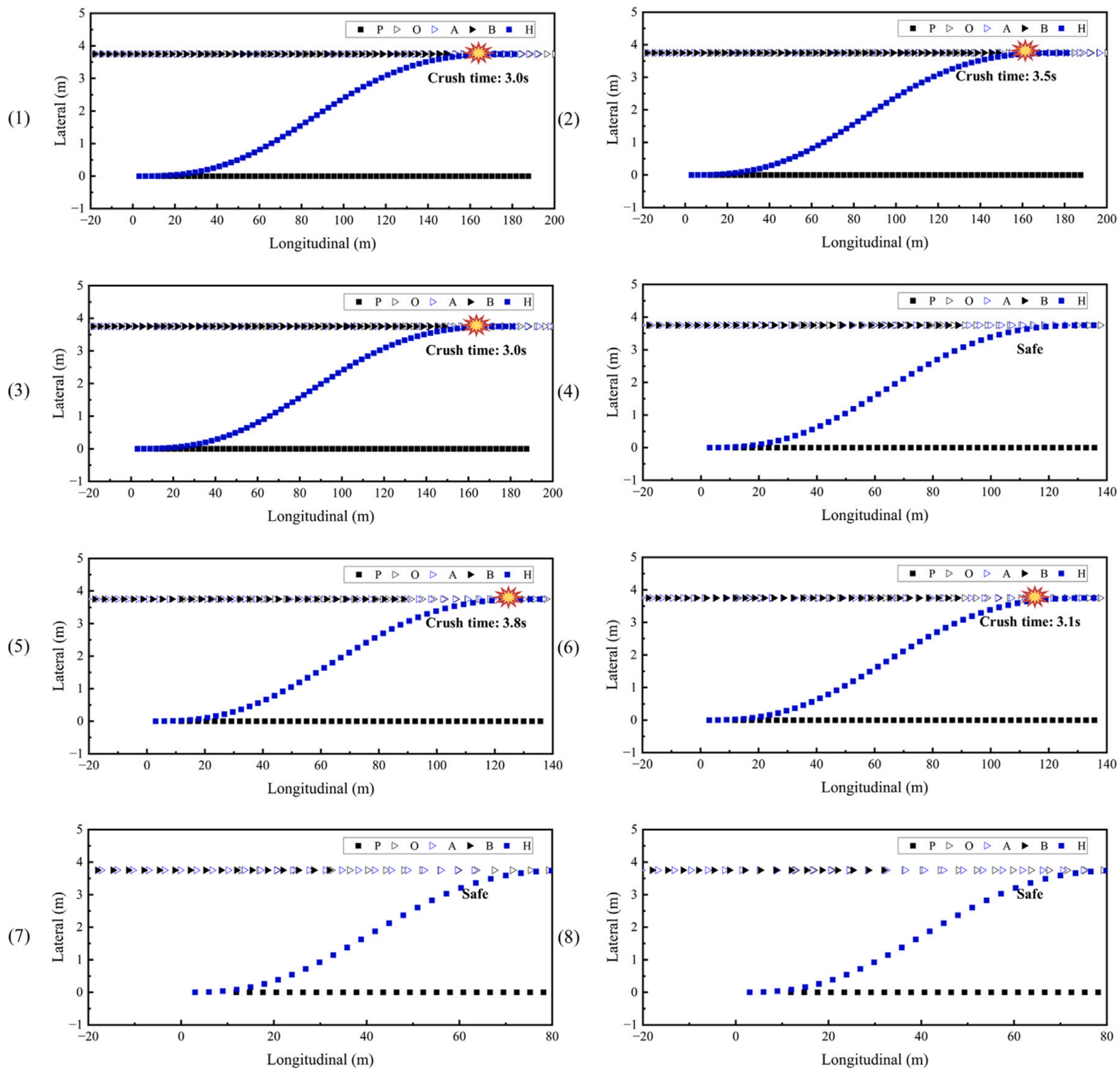

Fig. 18. 8 numerical original trajectory.

judgment effect is quite good. This DNN method has been shown to be practical. The second neural net is the fittest. Its use requires permission from the previous neural network. Its input matches the input of the DNN classifier. But the output is a novel polynomial trajectory curve. Since the coefficients of a quintic polynomial curve are complex and sensitive, the information about the endpoint of the quintic polynomial was used as the output of the analysis. Information about the endpoint primarily includes the LC time t of the new trajectory as well as the longitudinal displacement x of the LC. It has been tempting to use a simple neural network. There is only one hidden layer, and the number of hidden neurons is also set to 10. Levenberg Marquardt is used as a training method for this neural network. Meanwhile, its effect was good in an unexpected way. With a coefficient of determination of 0.996 for the entire test set. The coefficient of determination closer to 1, the greater the explanatory power of the variables in the equation for y, and this model also provides a good fit to the data. Closer to 0, the worse the model fits. We can see that the neural network adaptation effect is very good. In this work, a simple and efficient network were used. It should be noted that they do have room for improvement. For this reason, more alternative data-driven methods are welcome. But the present work first uses both of these models to analyze the effectiveness of LC trajectory re-planning models.

Table 4
Values of 8 numerical test conditions.

Case	Original time	Original distance	Acceleration
1	6.2 s	181 m	1 m/s^2
2	6.2 s	181 m	2.5 m/s^2
3	6.2 s	181 m	4 m/s^2
4	4.5 s	135.5 m	1 m/s^2
5	4.5 s	135.5 m	2.5 m/s^2
6	4.5 s	135.5 m	4 m/s^2
7	2.8 s	86.5 m	1 m/s^2
8	2.8 s	86.5 m	4 m/s^2

5. Validation of trajectory replanning

In the highway scenario, eight sets of scenarios were designed, with parameters shown in Table 4. The eight numerical test conditions cover three original trajectories and different value taking strategies, which are suitable for research comparison. For eight operating conditions, the original trajectory is shown in Fig. 18. In scenarios 1, 2, 3, 5, and 6, inter vehicle collision behaviors will occur under the originally planned LC trajectory, and the occurrence time is marked in Fig. 18.

Table 5
Risk response results during lane-changing for 8 test cases.

Case	Trigger	Original trajectory	Safety	4-point judge	New trajectory	New safety	Revised judge
1	0.7 s	6.2 s, 181.0 m	Dangerous	Return at 1.5 s	0.7 + 4.4 s, 144.5 m	Dangerous	Return at 0.7 s
1	1.6 s	6.2 s, 181.0 m	Dangerous	Return at 1.5 s	Return at 1.6 s	Safe	Return at 1.5 s
2	0.3 s	6.2 s, 181.0 m	Dangerous	Return at 1.5 s	0.3 + 7.3 s, 218.9 m	Safe	0.3 + 7.3 s, 218.9 m
2	0.6 s	6.2 s, 181.0 m	Dangerous	Return at 1.5 s	0.6 + 8.3 s, 254.3 m	Safe	0.6 + 8.3 s, 254.3 m
3	0.2 s	6.2 s, 181.0 m	Dangerous	Return at 1.5 s	0.2 + 6.8 s, 204.0 m	Safe	0.2 + 6.8 s, 204.0 m
3	0.4 s	6.2 s, 181.0 m	Dangerous	Return at 1.5 s	0.4 + 6.9 s, 207.7 m	Safe	0.4 + 6.9 s, 207.7 m
4	–	4.5 s, 135.5 m	Safe	Original Traj	Original Traj	Safe	Original Traj
5	2.5 s	4.5 s, 135.5 m	Dangerous	Return at 1.1 s	Return at 2.5 s	Safe	Return at 1.1 s
5	4.1 s	4.5 s, 135.5 m	Dangerous	Return at 1.1 s	Return at 4.1 s	Safe	Return at 1.1 s
6	1.0 s	4.5 s, 135.5 m	Dangerous	Return at 1.1 s	Return at 1.0 s	Safe	Return at 1.0 s
6	1.6 s	4.5 s, 135.5 m	Dangerous	Return at 1.1 s	Return at 1.6 s	Safe	Return at 1.1 s
7	–	2.8 s, 86.5 m	Safe	Original Traj	Original Traj	Safe	Original Traj
8	–	2.8 s, 86.5 m	Safe	Original Traj	Original Traj	Safe	Original Traj

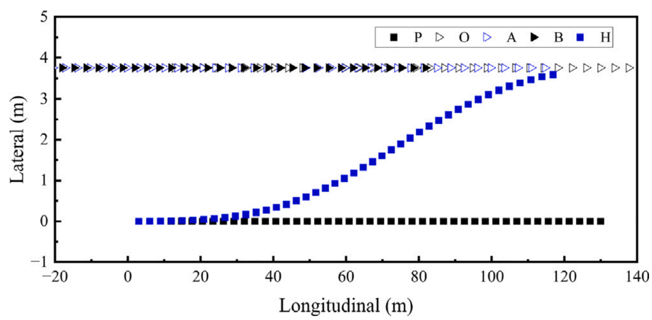

Fig. 19. Re-planned trajectory in numerical validation 1 with 0.7 s trigger time.

5.1. Performance comparison

To verify the feasibility and shortcomings of the proposed trajectory re-planning method, three comparative methods are proposed: original LC trajectory without considering safety, the model detecting safety at the four nodes of the transfer process, and return to the original lane as soon as possible if there is a danger, and the method trying to re-plan the LC trajectory as possible. The following numerical examples will be compared using these three processing ideas. The data and processing results of eight numerical cases are shown in Table 5. In the Table 5, safety represents the security of the original LC trajectory, judge represents response measures, and new safety represents the security of the new trajectory obtained through the NN method. Revised judge represents a response measure to integrate 4-point and NN methods.

For numerical validation 1, the current case is a scenario that may lead to collision behavior. Assuming that there are two types of delay times: 2 s and 5 s, the trajectory is re-planned twice, respectively. With 2 s as the delay time, the vehicle trigger is 0.7 s. The replanning model outputs a re-planned optimal LC trajectory, as shown in Fig. 19. It's new LC time is 5.05 (0.7 + 4.35) seconds, and the longitudinal position of the new LC target is 144.5 m. The behavior of early LC is selected compared to the original LC trajectory. However, Fig. 19 shows that the trajectory will still collide significantly with the vehicle in the 3.5 s of re-planning trajectory. This reflects a disadvantage of the data fitting model: Although it has high accuracy, it can still cause serious misjudgments. This issue is also mentioned in the first section of Chapter 4 of this work. In any practical case, when considering using a data fitting model, the security detection module is indispensable. The model proposed in this work adds a safety detection to the original model. The main process is to conduct collision analysis between the lane-change rescheduling trajectory curve and the trigger time predicted trajectory curve of vehicle A. If a collision is found, it is determined that the NN result is not credible, and the process of returning to the original lane is taken. Although only one case is discussed here, it can be found from Table 5 that the only scenario that can lead to a dangerous trajectory for re-planning is Case 1. And Case 1 is the only re-planning trajectory that attempts to achieve collision avoidance through acceleration. Correspondingly to the impact factor analysis section, the trajectory zone in Figs. 10(a) and 11(a) is extremely small, and the left and right sides of Figs. 14(a) and 14(b) are unbalanced. It shows that for LC trajectory re-planning, accelerating collision avoidance is difficult, and there are fewer samples available for training NN models, making it easier to produce inappropriate outputs. This situation may be improved with the support of a large amount of training data.

At 5 s, the vehicle trigger is 1.6 s. The model considers that it is not feasible to persist in LC behavior. When the vehicle does not have safety detection capability, the vehicle will collide at 3.0 s. When the vehicle detects a safe state using the 4 point method, it will plan its trajectory back to the original lane in 1.5 s. The re-planning module proposed in this work will trigger the behavior of returning to the original lane in 1.6 s. The difference between the return time of the 4-point method and the return time of the reprogramming module is mainly reflected in the decision-making time of risk judgment. The risk acceleration model proposed in Eq. (11) is not necessarily higher than the four-point model in sensing conflict type HV. The understanding of safety risks still depends on accurate environmental prediction and judgment criteria. Therefore, as shown in Table 5, to maximize the safety of LC, the revised re-plan module selects a smaller risk judgment time for both as the trigger time.

For numerical validation 2, the current case is a scenario that may lead to collision behavior. With 2 s as the delay time, the vehicle trigger is 0.3 s. The model outputs a re-planned optimal LC trajectory, as shown in Fig. 20(a). Its new LC time is 7.6 (0.3 + 7.3) s, and the longitudinal position of the new LC target is 218.9 m. At 5 s, the vehicle trigger is 0.6. The model outputs a re-planned optimal LC trajectory, as shown in Fig. 20. Its new LC time is 8.9 (0.6 + 8.3) s, and the longitudinal position of the new LC target is 254.3 m. In numerical validation 2, the proposed method of rapid re-planning of lane-change trajectory has a good effect. The basic conditions for lane-change trajectory design are ensured while adhering to change lane.

For numerical validation 3, At 2 s, the vehicle trigger is 0.2 s. The model outputs a re-planned optimal LC trajectory, as shown in Fig. 21(a). Its new LC time is 7.0 (0.2 + 6.8) s, and the longitudinal position of the new LC target is 204.0 m. At 5 s, the vehicle trigger is 0.4 s. At this point, the model outputs a re-planned optimal LC trajectory, as shown in Fig. 21(b). Its new LC time is 7.3 (0.4 + 6.9) s, and the longitudinal position of the new LC target is 207.7 m.

For numerical validation 4 & 7 & 8, those cases are a scenario where collision behavior is unlikely to occur. Therefore, the vehicle does not need to enter the processing stage of trajectory re-planning. Neither security response method will run a risk avoidance program. Numerical Validation 7 and 8 are typical fast LC scenarios with a safe distance left. In those 2 scenarios, even if vehicle A experiences an acceleration of 6 m/s^2, the vehicle currently undergoing LC will not be affected. Besides, the numerical validation 5 is a scenario that may lead to collision behavior. Assuming that there are two types of delay

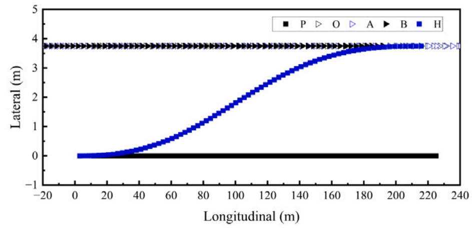

(a) Re-planned trajectory with 0.3 s trigger time

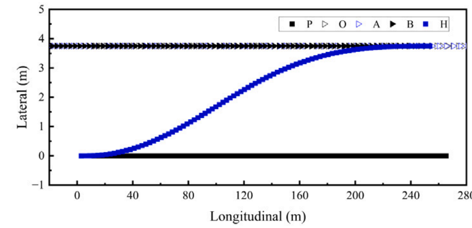

(b) Re-planned trajectory with 0.6 s trigger time

Fig. 20. Numerical validation 2.

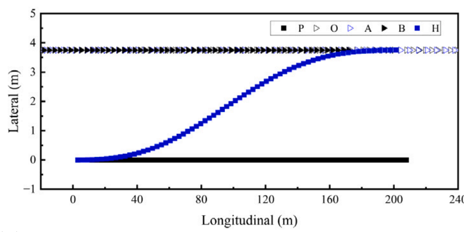

(a) Re-planned trajectory with 0.2 s trigger time

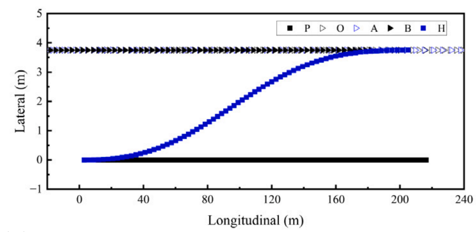

(b) Re-planned trajectory with 0.4 s trigger time

Fig. 21. Numerical validation 3.

times: 1.5 s and 2.5 s, the trajectory is re-planned twice, respectively. At 1.5 s, the vehicle trigger is 2.5 s. At 2.5 s, the vehicle trigger is 4.1 s. However, the model considers that it is not feasible to persist in LC behavior. Similarly, assuming that there are two types of delay times for case 6: 1.5 s and 2.5 s, the trajectory is re-planned twice, respectively. At 1.5 s, the vehicle trigger is 1 s. At 2.5 s, the vehicle trigger is 1.6 s. The 4-point method also chooses to return to the original lane as soon as possible to avoid risks.

Based on the above eight cases, in some scenarios, the method of using NN to re-plan the lane-change trajectory can be more flexible in dealing with safety issues caused by conflicting vehicles. Compared to the four-point method of returning to the original lane, it can persist in changing lanes under safe conditions, improving road traffic efficiency. At the same time, deficiencies based on neural networks and risk perception time have also been identified. Therefore, a safety check module has been added to the original model to prevent serious misjudgments in the data fitting model. It should be noted that the selected scenarios in this article are actually uncommon in reality for two main reasons. First, this work is predicated on the premise that vehicles encounter hazards during LC. In the case of an autonomous vehicle, this means that the environment is safe when the LC is initiated. So that belongs to sudden danger and is not in itself very common. Often, humans with a sense of road occupancy do not speed up too much. The focus of this article is on an extreme situation. Second, this work also presents numerous scenarios that do not require modification of the LC trajectory. The reason for this is that when a vehicle encounters such an unsafe situation, if it is too far away from it, it is often safe. As a result, the several test scenarios chosen in this paper have the potential for collisions, which may differ from common scenarios. In this scenario, LC trajectory re-planning is significant.

5.2. Real-time performance

To illustrate the real-time computing advantages of using NN as a data fitting model, numerical test cases 1, 2, and 3 were once again used for demonstration. Table 6 shows the calculation time differences between data fitting methods and traversal methods under different scenarios. The original time represents the time required to search for the optimal trajectory through traversal, the available trajectories represent the number of available trajectories in the trajectory area of the current case, the NN time represents the time required to use two neural network models, and the Revised NN time represents the time required to combine the neural network and security rules for the model. Time saving rate is the relationship between original time and revised NN time. The Intel i7-11700 CPU, Win 10 operating system and MATLAB software were consistently used for the calculation time test of this work.

It can be seen that although the traversal method can obtain all feasible trajectory numbers in detail and choose the best from them, its calculation time is too long and does not have real-time performance. In contrast, the performance of the data-fitting model NN is particularly excellent. Even if a safety check module is added after each operation, it can still basically achieve a calculation frequency of 10 Hz. Therefore, the lane-change trajectory re-planning method based on the data-fitting method is more feasible for actual road execution. To summarize, the four-point method is a simple rule-of-thumb empirical method with simple parameter settings, but there is still room for improvement. The neural network method has good real-time performance and can quickly generate re-planned trajectories, while not all neural networks can always generate reasonable trajectory curves. The modified neural network method combines the characteristics of both methods to ensure that the output of the neural network is verified. Meanwhile, its execution speed slightly decreases.

6. Conclusion

This study primarily focuses on building a real-time lane-changing trajectory re-planning module for vehicles, aiming to mitigate potential dangers during the lane-changing process. The research is based on the premise that vehicles face risks while changing lanes. Through a case study, it was found that four factors significantly affect the need for lane-changing trajectory re-planning: the original trajectory planning, trigger time, conflicting vehicle acceleration performance, and conflicting vehicle intent post-collision. To help vehicles efficiently determine the possibility of continuing the lane-change while avoiding risks, two neural network models were employed. These models were utilized to assess the feasibility of trajectory re-programming and to generate the optimal output trajectory. Through a numerical example, a comparison between the two methods demonstrates that the proposed data fitting-based lane-changing trajectory re-planning model exhibits reasonable real-time performance and feasibility. This approach considerably improves lane-changing efficiency and traffic capacity while maintaining road safety.

Table 6
Comparison of operation time for numerical test cases 1–3.

Cases	Trigger (s)	Original time (s)	Available trajectories	NN time (s)	Revised NN time (s)	Time saving rate (%)
1	0.7	2.699	149	0.059	0.105	96.10
1	1.6	2.447	2	0.069	0.116	95.27
2	0.3	3.369	419	0.023	0.070	97.92
2	0.6	3.233	34	0.084	0.130	95.97
3	0.2	3.902	1463	0.031	0.078	98.00
3	0.4	3.759	1279	0.032	0.079	97.90

There are two potential areas for further development in this study. First, in the context of wider roads, there may be opportunities for incorporating an intermediate state where vehicles momentarily straddle lane markings while waiting for an opening. Second, the trajectory design should consider an increased safety margin accounting for lateral distances. These two aspects form possible future research objectives. Our work may continue to explore these issues in the context of lane-changing trajectory re-planning.

CRediT authorship contribution statement

Haifeng Du: Methodology, Software, Formal analysis, Investigation, Writing – original draft. **Yu Sun:** Formal analysis, Data curation, Writing – original draft. **Yongjun Pan:** Conceptualization, Methodology, Writing – review & editing, Supervision, Funding acquisition. **Zhixiong Li:** Data curation, Visualization, Investigation, Validation. **Patrick Siarry:** Methodology, Writing – review & editing, Supervision.

Declaration of competing interest

The authors declare that they have no known competing financial interests or personal relationships that could have appeared to influence the work reported in this paper.

Data availability

The data that has been used is confidential.

Acknowledgments

This work was funded by the National Natural Science Foundation of China (No. 12072050 and No. 12211530029) and the Norwegian Financial Mechanism 2014-2021 under Project Contract No 2020/37/K/ST8/02748.

References

Ajanović, Z., Regolin, E., Shyrokau, B., Ćatić, H., Horn, M., Ferrara, A., 2023. Search-based task and motion planning for hybrid systems: Agile autonomous vehicles. Eng. Appl. Artif. Intell. 121, 105893.
Bae, S., Isele, D., Nakhaei, A., Xu, P., Añon, A.M., Choi, C., Fujimura, K., Moura, S., 2022. Lane-change in dense traffic with model predictive control and neural networks. IEEE Trans. Control Syst. Technol..
Chen, T., Cai, Y., Chen, L., Xu, X., 2022. Trajectory and velocity planning method of emergency rescue vehicle based on segmented three-dimensional quartic bezier curve. IEEE Trans. Intell. Transp. Syst..
Chhabra, R., Singh, S., Khullar, V., 2023. Privacy enabled driver behavior analysis in heterogeneous IoV using federated learning. Eng. Appl. Artif. Intell. 120, 105881.
Ding, Y., Zhuang, W., Wang, L., Liu, J., Guvenc, L., Li, Z., 2021. Safe and optimal lane-change path planning for automated driving. Proc. Inst. Mech. Eng. D 235 (4), 1070–1083.
Du, H., Pan, Y., Kawsar, I., Li, Z., Hou, L., Glowacz, A., 2023. Enhanced traffic safety and efficiency of an accelerated LC decision via DNN-APF technique. Measurement 217, 113029.
Fukuyama, S., 2020. Dynamic game-based approach for optimizing merging vehicle trajectories using time-expanded decision diagram. Transp. Res. C 120, 102766.
Guanetti, J., Kim, Y., Borrelli, F., 2018. Control of connected and automated vehicles: State of the art and future challenges. Annu. Rev. Control 45, 18–40.
Hu, W., Deng, Z., Cao, D., Zhang, B., Khajepour, A., Zeng, L., Wu, Y., 2022. Probabilistic lane-change decision-making and planning for autonomous heavy vehicles. IEEE/CAA J. Autom. Sin. 9 (12), 2161–2173.
Kim, C., Yoon, Y., Kim, S., Yoo, M.J., Yi, K., 2023. Trajectory planning and control of autonomous vehicles for static vehicle avoidance in dynamic traffic environments. IEEE Access.
Lee, K., Isele, D., Theodorou, E.A., Bae, S., 2022. Spatiotemporal costmap inference for mpc via deep inverse reinforcement learning. IEEE Robot. Autom. Lett. 7 (2), 3194–3201.
Li, Y., Li, L., Ni, D., Wang, W., 2022a. Automatic lane-changing trajectory planning: From self-optimum to local-optimum. IEEE Trans. Intell. Transp. Syst. 23 (11), 21004–21014.
Li, T., Wang, L., Liu, J., Yuan, J., Liu, P., 2022b. Sharing the roads: Robot drivers (vs. human drivers) might provoke greater driving anger when they perform identical annoying driving behaviors. Int. J. Hum.–Comput. Interact. 38 (4), 309–323.
Li, S., Wei, C., Wang, Y., 2022c. Combining decision making and trajectory planning for lane changing using deep reinforcement learning. IEEE Trans. Intell. Transp. Syst. 23 (9), 16110–16136.
Maleki, M., Taghavipour, A., Azadi, S., 2022. A real-time optimal cooperative lane change strategy via V2V communication. Proc. Inst. Mech. Eng. D 09544070221127123.
Nie, X., Min, C., Pan, Y., Li, K., Li, Z., 2022. Deep-neural-network-based modelling of longitudinal-lateral dynamics to predict the vehicle states for autonomous driving. Sensors 22, 2013.
Pan, Y., He, Y., Mikkola, A., 2019. Accurate real-time truck simulation via semirecursive formulation and Adams–Bashforth–Moulton algorithm. Acta Mech. Sinica 35, 641–652.
Pan, Y., Nie, X., Li, Z., Gu, S., 2021. Data-driven vehicle modeling of longitudinal dynamics based on a multibody model and deep neural networks. Measurement 180, 109541.
Pan, Y., Zhang, X., Liu, Y., Wang, H., Cao, Y., Liu, X., Liu, B., 2022. Dynamic behavior prediction of modules in crushing via FEA-DNN technique for durable battery-pack system design. Appl. Energy 322, 119527.
Rahman, M., Chowdhury, M., Xie, Y., He, Y., 2013. Review of microscopic lane-changing models and future research opportunities. IEEE Trans. Intell. Transp. Syst. 14 (4), 1942–1956.
Rhode, S., Van Vaerenbergh, S., Pfriem, M., 2020. Power prediction for electric vehicles using online machine learning. Eng. Appl. Artif. Intell. 87, 103278.
Schwarting, W., Alonso-Mora, J., Rus, D., 2018. Planning and decision-making for autonomous vehicles. Annu. Rev. Control, Robot., Auton. Syst. 1, 187–210.
Typaldos, P., Papageorgiou, M., Papamichail, I., 2022. Optimization-based path-planning for connected and non-connected automated vehicles. Transp. Res. C 134, 103487.
Wang, D., Wang, G., Wang, H., 2023. Optimal lane change path planning based on the NSGA-II and TOPSIS algorithms. Appl. Sci. 13 (2), 1149.
Yan, Y., Wang, J., Zhang, K., Liu, Y., Liu, Y., Yin, G., 2022. Driver's individual risk perception-based trajectory planning: A human-like method. IEEE Trans. Intell. Transp. Syst. 23 (11), 20413–20428.
Yang, C., Chen, X., Lin, X., Li, M., 2022a. Coordinated trajectory planning for lane-changing in the weaving areas of dedicated lanes for connected and automated vehicles. Transp. Res. C 144, 103864.
Yang, W., Li, C., Zhou, Y., 2022b. A path planning method for autonomous vehicles based on risk assessment. World Electr. Veh. J. 13 (12), 234.
Yu, Y., Luo, X., Su, Q., Peng, W., 2023. A dynamic lane-changing decision and trajectory planning model of autonomous vehicles under mixed autonomous vehicle and human-driven vehicle environment. Physica A 609, 128361.
Zhang, K., Chang, C., Zhong, W., Li, S., Li, Z., Li, L., 2022a. A systematic solution of human driving behavior modeling and simulation for automated vehicle studies. IEEE Trans. Intell. Transp. Syst. 23 (11), 21944–21958.
Zhang, S., Deng, G., Yang, E., Ou, J., 2022b. Optimal vehicle lane change trajectory planning in multi-vehicle traffic environments. Appl. Sci. 12 (19), 9662.
Zhang, X., Xiong, Y., Pan, Y., Du, H., Liu, B., 2023. Crushing stress and vibration fatigue-life optimization of a battery-pack system. Struct. Multidiscip. Optim. 66 (3), 1–16.
Zhang, Z., Zhang, L., Deng, J., Wang, M., Wang, Z., Cao, D., 2021. An enabling trajectory planning scheme for lane change collision avoidance on highways. IEEE Trans. Intell. Veh..